ANALITYCAL METHODS FOR THE ANAYSIS OF PHASE TRANSFORMATIONS IN SOLID STATE OCCURING DURING WELDING

PIEKARSKA Wiesława, GOSZCZYŃSKA Dorota

Częstochowa University of Technology, Institute of Mechanics and Machine Design Foundations, Częstochowa, Poland, EU

Abstract

Analytical models used for the analysis of phase transformations as well as the prediction of structural composition of welded elements are the subject of research for many years. Despite of certain simplifications they are invaluable in assessing the weldability and welding conditions. Results obtained by analytical methods are often used for the initial analysis of the material properties prior to the experimental studies and used before developing of mathematical models.

The paper presents an analysis of phase transformations in solid state during welding of S460 steel. Empirical relations are given with the cooling rates taken into consideration, on which start and finish temperatures of bainite, ferrite pearlite, and martensite transformation are determined. Obtained data allowed predicting different start and finishing temperatures of phase transformations for various cooling rates $v_{8/5}$ ($t_{8/5}$). Analytical Continuous-Cooling-Transformation (CCT) diagram for steel is determined as well as volume fractions of phases in a function of cooling rates. Analytically obtained results are compared with experimental data obtained by dilatometric tests.

Keywords: Analytical methods, phase transformations, heat affected zone, phase volumetric fractions

1. INTRODUCTION

Material changes its thermophysical and mechanical properties during welding, due to alternating temperature field in a wide range. Particularly different material properties occur in heat affected zone (HAZ). In HAZ a large variety of structures occurs conditioned by thermal cycles as a result of phase transformations in solid state. Analytical models concern prediction of HAZ structure on the basis of chemical composition of steel as well as elaboration of simplified CCT diagrams and estimation of mechanical properties of HAZ in welded joints [2, 6, 8]. Most often averaged values are assumed, which reduces the accuracy of models in the analysis of particular materials and specific welding technology. Against these limitations, analytical formulas are invaluable in assessing the weldability and welding conditions as an alternative of labor-intensive technology research. Particularly, the use of the combined analytical methods [1-8] and results of numerical analysis could be useful in a wide range of scientific applications [9-11].

2. MATHEMATICAL MODELS OF PHASE TRANSFORMATIONS, ANALYTICAL AND EXPERIMENTAL CCT DIAGRAMS

Analytical models created on the basis of the chemical composition of steel are used to predict phase distributions in HAZ, further to develop simplified CCT diagrams. Equations are obtained by the use of statistical analysis of results of experimental research performed for certain material groups. These relationships concern characteristic values such as: start and finish temperatures and times of phase transformations during heating and cooling, cooling rates as a function of the heat source power and critical cooling rates wherein hardening structures are present [2, 3, 4, 6]. S460 steel belongs to a group of weldable low carbon and high strength steels. Selected analytical dependencies presented in this paper are refer to this

type of steel. Chemical composition of steel S460 is shown in **Table 1**. Symbols of chemical elements were provided by all empirical formulas and means percentage of a given element, e.g. C→%C.

Table 1 Chemical composition of S460 steel In %

Steel	C	Mn	Si	Cr	Ni	Cu	V	Al	Nb
S460	0.19	1.62	0.60	0.10	0.09	0.11	0.10	0.032	0.012

In order to create analytical CCT diagram two different analytical models are used in this work. Two used models have different approaches in determining the time of initiation of austenite transformation with respect to chemical composition of steel. Start and finish temperatures of each phase transformation are determined for start and finish times of phase transformations estimated in relation to chemical composition of analysed steel. Presented models are developed for austenitizing temperature 1300 °C.

Time $t_{8/5}$ and initialization times of diffusive transformations as: bainite t_B, ferrite t_F and perlite t_P are described by model I [3] and model II [2], expressed as follows:

Model I:

$$\ln t_B = -2.4 + 0.45\sqrt{C} + 0.91Mn + 0.37Si + 0.57 + 0.91Mo + 0.75Ni \quad (1)$$

$$\ln t_F = -3.3 + 6.9\sqrt{C} + 2.0Mn + 1.52Cr + 2.66Mo - 3.76V \quad (2)$$

$$\ln t_P = 0.825 + 1.64Mn + 0.76Si + 1.64Cr + 2.17Mo + 0.94N \quad (3)$$

$$\ln t_k = -0.07 + 0.84Mn + 1.40Cr + 3.35\sqrt{C} \quad (4)$$

Model II:

$$t_B = \exp(7.4(C + Si/24 + (Mn + Cr)/6 + Cu/15 + Ni/40 + Mo/4 + (Nb + V)/5 + 5B) - 3.027) \quad (5)$$

$$t_F = 10^{[5.8(C+Si/291+Mn/14+Ni/67+Cr/16+Mo/6+V/425)-0.83]} \quad (6)$$

$$t_P = 10^{[5.14(C+Si/17+Mn/19+Ni/25+Cr/16+Mo/4+V/3)+0.06]} \quad (7)$$

where t_B, t_F, t_P are start times of bainite, ferrite and pearlite transformations respectively, whereas t_k is the finish time.

Time-dependent ($t = t_{8/5}$) start temperatures of the formation ferrite $F_s(t)$, bainite $B_s(t)$, pearlite $P_s(t)$ and the finish temperature of phase transformations $T_k(t)$ are determined by formulas [3, 4], in the following form:

$$B_s(t) = T_{B0} + \Delta T_B erf[(\ln t - \ln t_{B0})K_B] + K_{Bt}\ln t \rightarrow T_{B0} = T_{B0}(t) = M_s$$

$$F_s(t) = T_{F0} + \Delta T_F erf[(\ln t - \ln t_{F0})K_F] + K_{Ft}\ln t \rightarrow T_{k0} = T_{k0}(t) = M_s \quad (8)$$

$$P_s(t) = T_{P0} + \Delta T_P erf[(\ln t - \ln t_{P0})K_P] + K_{Pt}\ln t \rightarrow T_{F0} = B_s(t_{F0})$$

$$T_k(t) = T_{k0} + \Delta T_k erf[(\ln t - \ln t_{k0})K_k] + K_{kt}\ln t \rightarrow T_{P0} = B_s(t_{P0}) \quad (9)$$

values: $\Delta T_B, \Delta T_{Bt}, \Delta T_F, \Delta T_{Ft}, \Delta T_P, \Delta T_{Pt}, \Delta T_k, \Delta T_{kt}$ depend on the chemical composition of investigated steel [3,4].

Start temperature of martensite transformation, by model I and model II are described respectively [2, 6], Whereas finish temperature of martensite transformation M_f is defined by a widely used formula [2]:

$$M_s = 506 - 37C - 24.2Mn - 14.4Si - 14.7Ni + 214Nb \quad (10)$$

$$M_s = 646.6 - 4218.2C + 219.6Mn - 454Si + 41.4Cr - 134.7Ni + 9.3Mo - 7.1V + 35.2Nb + 2115.1C^2 - 175.3Mn^2 - 36.7Si^2 + 45.3Cr^2 + 95.5Ni^2 + 119.2Mo^2 + 716CMn + 228.6MnSi + 535.5CSi \quad (11)$$

$$M_f = 381.76 - 252.44C - 111.12Mn + 54.538Si + 114.17Cr - 23.779Ni - 57.381Mo + 215.7V + 945.4Nb + 1821.7Ti - 1746.5B \quad (12)$$

Dilatometric research on S460 steel is performed in order to verify obtained analytical results and to evaluate the usefulness of created diagram of austenite transformation. Dilatometric research is performed using DIL805 Bahr Thermoanalyse GmbH dilatometer. Austenitization temperature T_A=1200 °C and heating rate 100 K/s are assumed in dilatometric research as well as different cooling rates simulating thermal cycles in welding [11].

Analytical CCT diagrams of S460 steel obtained in formulas (1-12) and CCT diagram obtained by experimental research are presented in **Fig. 1**. Experimental CCT diagram is given as a comparison [11].

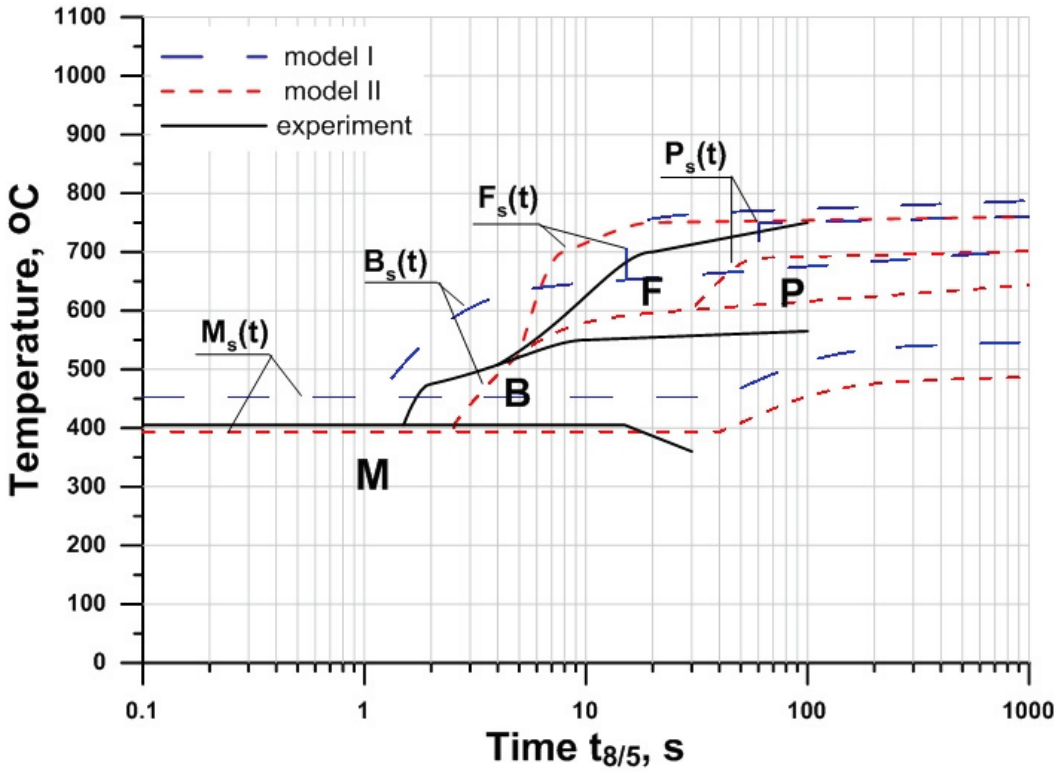

Fig. 1 CCT diagrams of S460 steel

Analytical models for determining phase composition with the dependence on cooling rates taken into account are very useful in phase transformation analysis. Equations that can be used to determine structural composition of steel in ambient temperature as a function of cooling time $t_{8/5}$ are shown in papers [2, 3]. Volume fractions of particular phases, such as: ferrite+pearlite, bainite and martensite, as a function of time $t_{8/5}$ are described as follows:

$$\eta_M = 0.5[1 - erf\frac{((\ln t) - \ln \Delta t_{FP})}{\ln S_{FP}}]; \quad \eta_{FP} = 0.5[1 + erf\frac{((\ln t) - \ln \Delta t_M)}{\ln S_M}]; \quad \eta_B = 1 - \eta_M - \eta_{FP} \tag{13}$$

where:

$$\ln \Delta t_{FP} = 0.85 + 7.43C + 1.84Mn + 0.55Cr + 3.2Mo + 0.95Ni - 9.26C^2$$

$$\ln S_{FP} = 1.42 - 1.6C + 0.23Mn + 0.42Si + 0.22Ni + 0.32Mo$$

$$\ln \Delta t_M = -1.49 + 13.6C + 1.0Mn + 0.33Si + 0.48Cr + 0.94Mo + 0.87Ni - 14.2C^2$$

$$\ln S_M = 0.65 - 0.52C + 0.23Mn + 0.16Cr + 0.18Mo$$

where Δt_{FP}, Δt_M are predicted cooling times in the temperature 800 °C to obtain 50 % fraction of ferrite-pearlite or martensite phase, $t=\Delta t_{8/5}$ is a cooling time in the temperature range 800-500 °C.

3. EXEMPLARY PREDICTION OF STRUCTURAL COMPOSITION

The electric arc butt-welding of S460 steel sheets with dimensions 150x30x3 mm is considered in this paper. Temperature field generated by moveable heat source is determined using ABAQUS/Standard [12]. The analysis of thermal phenomena is made on the basis of the solution of energy conservation equation together with Fourier law. Heat transfer differential equation is expressed in the weighted residuals criterion method. Governing equation is completed by initial and boundary condition of Dirichlet, Neumann and Newton type with heat loss due the convection and radiation [11].

Movable welding source is implemented in ABAQUS FEA [12] using additional numerical DFLUX subroutine. Used in this work mathematical model of surface, double-elliptical heat source (depth of the source z=0) is known as Goldak's heat source power distribution (**Fig. 2a**) [13]. In calculations of temperature field the following technological parameters are used: power of the electric arc Q=2200 [W] and welding speed v=9 [mm/s]. Exemplary welding heat source power distribution is shown in **Fig. 2b**.

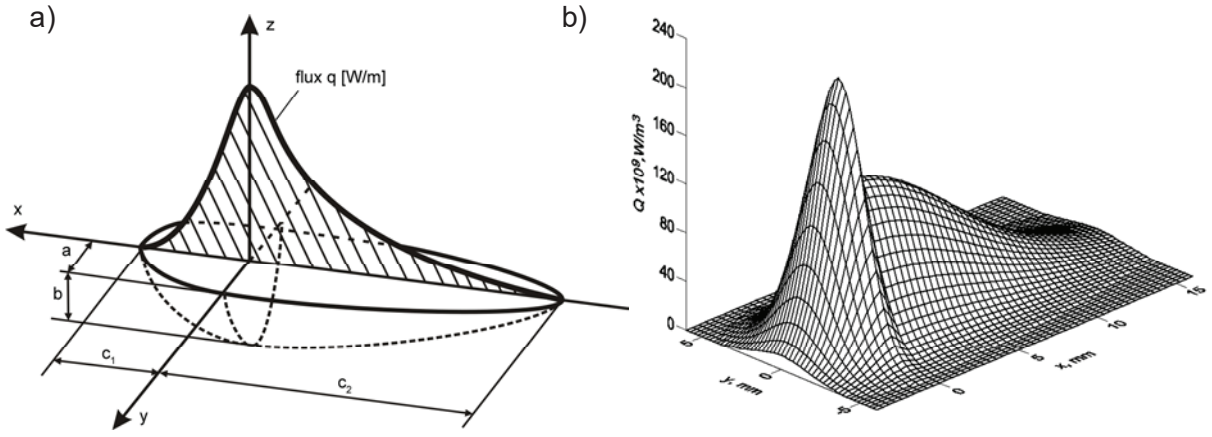

Fig. 2 Goldak's heat source model, a) the spatial model, b) exemplary power distribution

Cross section of considered welded joint, analyzed as 3D task, is presented in **Fig. 3**, with shown analysed material points. In this figure a fusion zone boundary is presented by a solid line (solidus isotherm), whereas dashed line illustrates HAZ boundary (austenizing temperature) Temperature distribution in the central layer at different distances from the axis of the source are presented in **Fig. 4** with characteristic $t_{8/5}$ times (**Fig. 3**). The analysis of phase transformations is performed on the basis of determined temperature distributions.

Results of the analysis are presented in the cross section of the weld for chosen material points at various distances from the weld line (points 1, 2, 3 and 4).

The prediction of structural composition in the weld and HAZ is performed on the basis of calculated volumetric fractions of phases in a function of time $\Delta t_{8/5}$. Results of the analytical prediction with the results of experimental research are shown in **Fig. 4**.

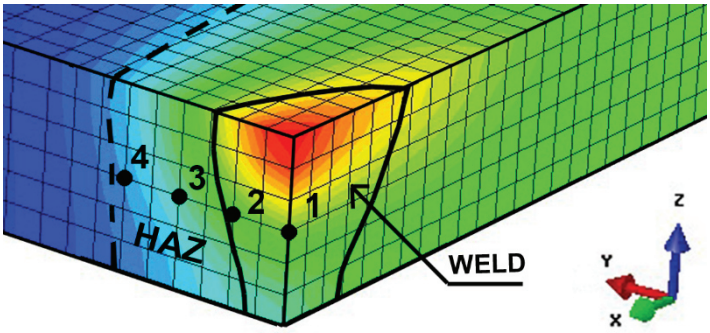

Points	1	2	3	4
Distance from the weld line, y [mm]	0	1	2	3
Time, $t_{8/5}$, [s]	7	7.5	8	8.5

Fig. 3 Temperature distribution in the cross-section of considered welded joint

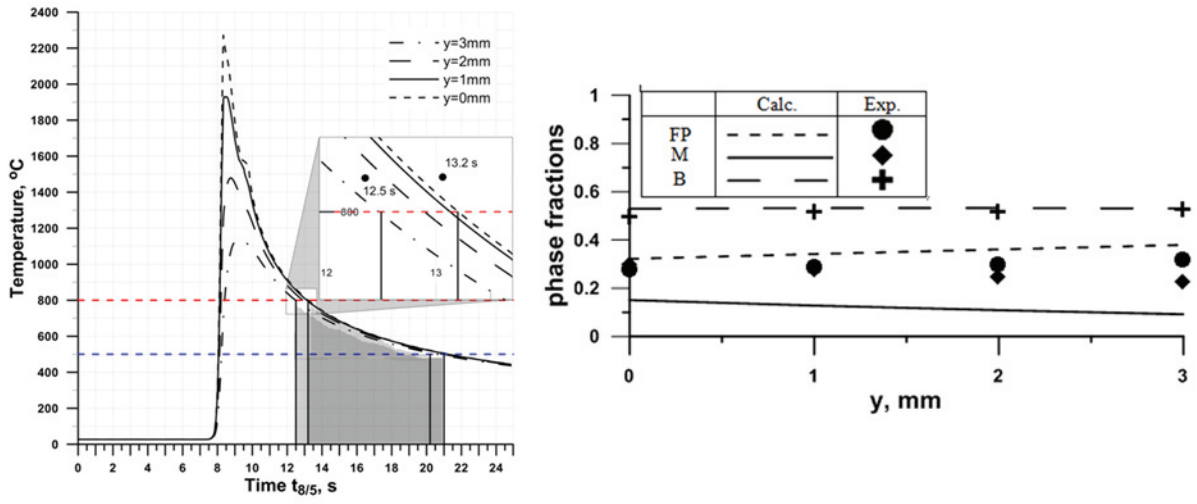

Fig. 4 Temperature distributions and phase fractions at different distances from the centre of the heat source

5. CONCLUSION

Analytical methods are very useful tool for the creation of simplified CCT diagrams and for predicting HAZ structure. They can be used as a cheap tool for assessing microstructure of the weld and in consequence mechanical properties of welded joints. The accuracy of the assessment is a major problem. In this paper usefulness of CCT diagrams and formed microstructure has been assessed. Comparison of analytical CCT diagrams (model I and model II) with diagram obtained by experimental research (**Fig. 1**) lead to the fact that empirical relationships properly reflect the decomposition of austenite phenomena.

Summarizing analytically obtained results, it can be concluded that analytical models with high accuracy can be used for creating CCT diagrams which largely identify with experimental results for steel research. Model I

a little more accurately reflects CCT diagrams. Present differences in comparison to the real diagram may be due to different austenitizing temperature of the experiment (1200°C) and presented models (1300°C).

Structure composition in the weld and HAZ of welded joints can be predicted on the basis of analytical estimation of volumetric fractions of phases and CCT diagram. During the analysis of the comparison of calculated phase fractions with results of experimental research (**Fig. 4**) distributions of diffusive phases of ferrite + pearlite and bainite exhibits great conformation with the results of experimental research are observed. Great conformation is not present when decomposition of martensite occurs. Mathematical models of the formation of these phases should be further analysed and verified on the basis of experimental studies for considered group of steel.

REFERENCES

[1] PERRET W., SCHWENK C., RETHMEIER M. Comparison of analytical and numerical welding temperature field calculation. Computational Materials Science, Vol. 47, 2010, 1005-1015.

[2] MIKUŁA J. Analityczne metody oceny spawalności stali. zeszyty naukowe Mechanika nr 85, Politechnika Krakowska, Kraków, 2001.

[3] SEYFFARTH P., KASATKIN O. G. Mathematisch-statistische Beschreibung der Austenitumwandlung in der Wärmeeinflußzone. Schweißtechnik, Vol. 29, 1979, pp. 117-119.

[4] KASATKIN O. G., SEYFFART P. Interpolâcionnye modeli dlâ ocenki fazovogo sostava zony termičeskogo vliâniâ pri dugovoj svarke nizkolegirovannyh stalej. Avtomat. Svarka, Vol. 1, 1984, pp. 7-11.

[5] MITTEMEIJER E.J., SOMMER F. Solid state phase transformation kinetics: a modular transformation model. Z. Metallkd, Vol. 93, 2002, pp. 352-360.

[6] PIEKARSKA W., Analiza numeryczna zjawisk termomechanicznych procesu spawania laserowego. Pole temperatury, przemiany fazowe i naprężenia. Seria Monografie nr 135, Wydawnictwo Politechniki Częstochowskiej, Częstochowa, 2007.

[7] TASAK E. Metalurgia spawania. wyd. JAK, Kraków, 2008.

[8] SHEN H., SHI Y., YAO Z., HU J. An analytical model for estimating deformation in laser forming. Computational Materials Science, Vol. 37, 2006, pp. 593-598.

[9] WINCZEK J., RYGAŁ G. Modelling of a temporary temperature field during arc weld surfacing of steel elements taking into account heat of the weld. J. Appl. Math. Comput. Mech, Vol. 14, 2015, pp. 111-120.

[10] FRANCO A., ROMOLI L., MUSACHIO A. Modelling for predicting seam geometry in laser beam welding of stainless steel. International Journal of Thermal Sciences, Vol. 79, 2014, pp. 194-205.

[11] PIEKARSKA W., KUBIAK M., Theoretical investigations into heat transfer in laser-welded steel sheets. J. Therm. Anal. Calorim., Vol. 110, 2012, pp. 159-166.

[12] SIMULIA Dassault System. Abaqus theory manual, Version 6.7, 2007.

[13] GOLDAK J. A. Computational Welding Mechanics. Springer NY 2005.